THE JOURNAL OF BIOLOGICAL CHEMISTRY VOL. 282, NO. 40, pp. 29514–29520, October 5, 2007

Exploring the Ubiquinone Binding Cavity of Respiratory Complex I*[S]

Received for publication, June 1, 2007, and in revised form, July 16, 2007 Published, JBC Papers in Press, August 6, 2007, DOI 10.1074/jbc.M704519200

Maja A. Tocilescu, Uta Fendel, Klaus Zwicker, Stefan Kerscher, and Ulrich Brandt[1]

From the Johann Wolfgang Goethe-Universität, Fachbereich Medizin, Zentrum der Biologischen Chemie, Molekulare Bioenergetik, Centre of Excellence Frankfurt "Macromolecular Complexes", D-60590 Frankfurt am Main, Germany

Proton pumping respiratory complex I is a major player in mitochondrial energy conversion. Yet little is known about the molecular mechanism of this large membrane protein complex. Understanding the details of ubiquinone reduction will be prerequisite for elucidating this mechanism. Based on a recently published partial structure of the bacterial enzyme, we scanned the proposed ubiquinone binding cavity of complex I by site-directed mutagenesis in the strictly aerobic yeast *Yarrowia lipolytica*. The observed changes in catalytic activity and inhibitor sensitivity followed a consistent pattern and allowed us to define three functionally important regions near the ubiquinone-reducing iron-sulfur cluster N2. We identified a likely entry path for the substrate ubiquinone and defined a region involved in inhibitor binding within the cavity. Finally, we were able to highlight a functionally critical structural motif in the active site that consisted of Tyr-144 in the 49-kDa subunit, surrounded by three conserved hydrophobic residues.

Respiratory chain NADH:ubiquinone oxidoreductase (complex I) is a large membrane protein complex that catalyzes electron transfer from NADH to ubiquinone and thereby pumps protons across the inner mitochondrial or bacterial plasma membrane (1). Electron microscopy revealed that complex I is L-shaped (2–9) and is composed of a hydrophobic arm embedded in the membrane and a peripheral arm protruding into the mitochondrial matrix or the bacterial cytosol. The peripheral arm contains all known redox centers, one FMN and eight or nine iron-sulfur clusters. Based on sequence comparisons (10, 11), mutational analysis (12–15), and photoaffinity labeling studies (16), we have proposed previously (14, 17) that the PSST and the 49-kDa subunit that are homologous to the small and large subunit of [NiFe] hydrogenases form part of the quinone reducing catalytic core of complex I (note that the bovine nomenclature will be used for the central subunits of complex I throughout). Recently the crystal structure of the peripheral domain of complex I from *Thermus thermophilus* has been solved at 3.3 Å resolution (18). This structure (Fig. 1) shows a wire of iron-sulfur clusters connecting the NADH-binding site near FMN with a broad cavity formed by the PSST and the 49-kDa subunit that should comprise the active site for ubiquinone reduction and the binding region for the large number of inhibitors that have been found for complex I (19).

Because reduction of ubiquinone is likely to be a key event in the energy-coupling mechanism of complex I (1, 20), the quinone-binding site in the PSST and the 49-kDa subunit next to iron sulfur-cluster N2 is of particular interest. To identify the domains essential for catalytic activity and inhibitor binding, we introduced a set of point mutations in the PSST and the 49-kDa subunits of complex I from our model organism, the strictly aerobic yeast *Yarrowia lipolytica*. Positions for point mutations were chosen by analyzing the *T. thermophilus* structure so that they would probe all parts of the proposed quinone binding cavity and some surrounding residues.

EXPERIMENTAL PROCEDURES

Strains and Site-directed Mutagenesis—The *Y. lipolytica* *nucm*Δ and *nukm*Δ deletion strains described earlier (21, 22) were transformed with the replicative plasmids pUB26 containing a genomic fragment of the *NUCM* gene or pUB4 containing a genomic fragment of the *NUKM* gene. All point mutations were generated in *Escherichia coli* by PCR mutagenesis. After transformation (23) into *Y. lipolytica* strain *nucm*Δ or *nukm*Δ, plasmids were recovered, and the entire open reading frames were sequenced to verify the introduced point mutations and exclude other sequence changes.

Small Scale Preparation of Mitochondrial Membranes—Mitochondrial membranes were isolated essentially according to published protocols (24). After phenylmethylsulfonyl fluoride was added to a final concentration of 2 mM, mitochondrial membranes were homogenized, shock-frozen, and stored in liquid nitrogen. Aliquots of preparations were used for activity measurements and gel electrophoresis. Protein concentration was determined colorimetrically using the DC protein assay (Bio-Rad).

Measurement of Catalytic Activity—NADH:HAR[2] oxidoreductase activity was measured as NADH oxidation ($\epsilon_{340-400\,nm} = 6.22$ $mM^{-1}\,cm^{-1}$) in the presence of the artificial electron acceptor HAR using a Molecular Devices SPECTRAmax PLUS^{384} plate reader spectrometer. The activity was measured at 30 °C in 20

* This work was supported by the Deutsche Forschungsgemeinschaft SFB472, Project P2. The costs of publication of this article were defrayed in part by the payment of page charges. This article must therefore be hereby marked "*advertisement*" in accordance with 18 U.S.C. Section 1734 solely to indicate this fact.

[S] The on-line version of this article (available at http://www.jbc.org) contains supplemental Figs. S1 and S2.

[1] To whom correspondence should be addressed: Universität Frankfurt, Zentrum der Biologischen Chemie, Molekulare Bioenergetik, Theodor-Stern-Kai 7, Haus 26, D-60590 Frankfurt am Main, Germany. Tel.: 49-69-6301-6926; Fax: 49-69-6301-6970; E-mail: brandt@zbc.kgu.de.

[2] The abbreviations used are: HAR, hexaammineruthenium(III)-chloride; DBQ, *n*-decylubiquinone; dNADH, deamino-NADH (reduced form); DQA, 2-decyl-4-quinazolinylamine; Mops, 3-(*N*-morpholino)propanesulfonic acid.

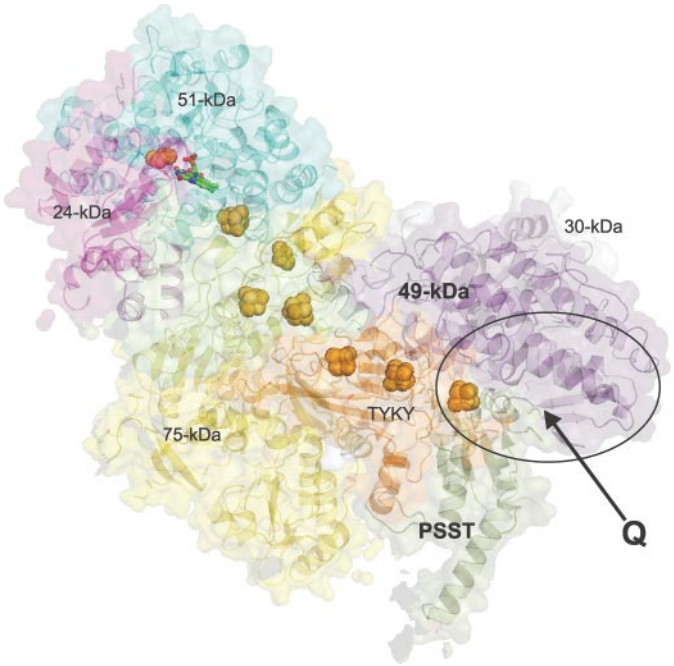

FIGURE 1. **Overall structure of the peripheral arm of *T. thermophilus* complex I.** The subunits are labeled according to the names introduced for bovine heart complex I. Only the eight iron-sulfur clusters found in bacterial and mitochondrial complex I are shown as space fill models. FMN is shown in *green* as a stick model. The putative access path for ubiquinone (*Q*) is indicated by an *arrow*, and the region that underwent mutagenesis in this study is highlighted by the *oval*.

mM Na^+/Hepes, pH 8.0, with 250 mM sucrose, 2 mM NaN_3, 0.2 mM EDTA, 0.2 mM NADH, and 2 mM HAR. The reaction was initiated by the addition of mitochondrial membranes (final concentration 25 μg of protein per ml). Specific NADH:HAR oxidoreductase activity was used to estimate complex I content because it is not affected by changes in the ubiquinone binding pocket.

dNADH:DBQ oxidoreductase activity of mitochondrial membranes was determined as the fraction of dNADH oxidation activity ($\epsilon_{340-400\ nm}$ = 6.22 mM^{-1} cm^{-1}) sensitive to the complex I inhibitor DQA in the presence of DBQ as electron acceptor. Measurements were carried out on a SPECTRAmax PLUS^{384} plate reader spectrometer (Molecular Devices) at 30 °C in 20 mM Na^+/Mops, pH 7.4, with 50 mM NaCl, 2 mM KCN, 0.1 mM dNADH, and 0.07 mM DBQ. The final concentration of mitochondrial membranes was 50 μg/ml. The reaction was started by adding DBQ. The inhibitor-sensitive fraction of the ubiquinone reductase activity was calculated by subtracting the residual rate in the presence of 27 μM DQA that was usually 5–10% of the dNADH:DBQ oxidoreductase activity of the parental strain. To allow comparison between different membrane preparations, all activities were normalized for complex I content. The results are given as mean ± S.E. (n = 5–15).

I_{50} values and apparent K_m values were determined under essentially the same conditions as dNADH:DBQ oxidoreductase activity by varying the inhibitor and DBQ concentrations, respectively. The I_{50} value is defined as the concentration of inhibitor that decreased the inhibitor-sensitive complex I activity by 50%. For determination of the apparent K_m, data were fitted using the program "Enzfitter" (version 2.0.17.0, Biosoft 1999, Cambridge, UK) and a modified Michaelis-Menten equation (25).

Gel Electrophoresis—Blue-native PAGE was carried out according to Schägger (26). Complex I in gel activity was preformed as described previously (27).

EPR Spectroscopy—X-band EPR spectra were obtained with a Bruker ESP 300E spectrometer equipped with an HP 53159A frequency counter (Hewlett Packard), ER 035 M NMR gaussmeter (Bruker, BioSpin), and a liquid helium continuous flow cryostat (Oxford Instruments). Spectra were recorded using the following parameters: microwave frequency 9.47 GHz, microwave power 5 milliwatts, modulation amplitude 0.64 millitesla, and modulation frequency 100 kHz.

Mitochondrial membranes (10–25 mg/ml, depending on the specific mutant) were reduced with 2 mM NADH or 2 mM NADH, 5 mM sodium dithionite. Samples were frozen in cold isopentane/methylcyclohexane (5:1, ~120 K) and stored in liquid nitrogen. Usually, spectra were recorded at temperatures of 40 K to analyze binuclear clusters only or at 12 K to analyze binuclear and tetranuclear clusters.

Structure Images—Images of the structural model and interpretation of the results from mutagenesis were based on the x-ray structure of the peripheral arm of complex I from *T. thermophilus* at 3.3 Å resolution (18). The software package PyMol (version 0.99) was used for visualizing the coordinates (Protein Data Bank 2FUG) and preparing the figures in which the amino acids were labeled using *Y. lipolytica* numbering that was deduced from aligning the sequences from the two organisms (supplemental Fig. S1). In cases where a residue was not conserved between *T. thermophilus* and *Y. lipolytica*, the side chain was exchanged to match the *Y. lipolytica* sequence using the mutagenesis wizard of the PyMol package.

RESULTS

Mutations in the Ubiquinone Binding Cavity Did Not Interfere with Complex I Assembly—To gain more insight into the function of amino acid residues that line the putative ubiquinone binding pocket (18), we generated a set of 39 point mutations covering 20 different residues of the 49-kDa and the PSST subunits of complex I from *Y. lipolytica* (Tables 1 and 2). In many positions the residues were exchanged by several different amino acids and at least one conservative, and one more drastic exchange was introduced if possible. Tables 1 and 2 also list data on point mutations that we had generated and analyzed before (14, 21, 22, 28), providing information on a total of 52 mutations at 26 positions. Mitochondrial membranes were isolated from all newly generated mutant *Y. lipolytica* strains, and complex I content was estimated as NADH:HAR oxidoreductase activity (Tables 1 and 2) and by blue-native PAGE with subsequent complex I in gel activity stain (data not shown). Membranes from most mutants contained fully assembled complex I in amounts comparable with the parental strain indicating that complex I was not destabilized in these mutants. Only very few mutations led to moderately decreased complex I contents, but even in these mutants complex I appeared to be fully assembled.

TABLE 1

Effects of point mutations introduced into the 49-kDa subunit

ND indicates not determined.

Strain	Complex I content[a]	Complex I activity[b]	Apparent K_m (DBQ)	I_{50} DQA	I_{50} Rotenone
	%	%	μM	nM	
Parental	100 ± 3	100 ± 5	15	16	530
A94I	85 ± 3	14 ± 2	ND	ND	ND
H95A[c]	130	<5	ND	ND	ND
H95M[c]	120	<5	ND	ND	ND
H95R[c]	100	<5	ND	ND	ND
V97W	78 ± 2	10 ± 2	ND	ND	ND
L98F	101 ± 3	22 ± 2	ND	ND	ND
L98K	71 ± 2	15 ± 2	ND	ND	ND
R99D	58 ± 2	14 ± 2	ND	ND	ND
R99T	71 ± 1	15 ± 2	ND	ND	ND
R141K[c]	140	45	13	55	1500
R141A	130[d]	17[d]	10[e]	21[d]	570[d]
Y144W	129 ± 2	8 ± 4	ND	ND	ND
Y144H[d]	70	<5	ND	ND	ND
V145F	127 ± 1	7 ± 3	ND	ND	ND
V145T	122 ± 4	92 ± 8	12	17	550
S146C[f]	100	100	12	80	1500
M188Y	104 ± 2	12 ± 2	ND	ND	ND
S192I	110 ± 3	16 ± 2	ND	ND	ND
S192R	102 ± 5	8 ± 2	ND	ND	ND
S192Y	111 ± 2	24 ± 2	ND	ND	ND
F207W	99 ± 2	58 ± 2	12	21	850
R210I	100 ± 2	63 ± 2	14	16	500
E211Q	124 ± 4	83 ± 6	16	21	530
E218Q	97 ± 2	97 ± 4	12	21	550
R224D	97 ± 2	107 ± 4	13	12	550
R224I	93 ± 3	102 ± 5	14	12	650
R224K	86 ± 2	103 ± 3	10	11	550
R224N	124 ± 2	99 ± 7	14	15	700
L225A	102 ± 3	103 ± 6	13	13	550
L225F	95 ± 3	110 ± 6	13	11	460
L225H	84 ± 3	107 ± 5	12	14	700
L225V	95 ± 2	91 ± 3	12	12	700
K407H	80 ± 2	78 ± 2	13	13	500
K407R	93 ± 3	105 ± 4	12	75	550
K407W	66 ± 1	12 ± 2	ND	ND	ND
G455I	71 ± 3	16 ± 2	ND	ND	ND
G455S	98 ± 1	72 ± 4	11	22	700
D458A	93[d]	28[d]	12[e]	520[d]	5200[d]
L459I	92 ± 7	92 ± 10	16	13	620
L459K	50 ± 2	24 ± 2	ND	ND	ND
V460A[d]	90	<5	ND	ND	ND
V460L	83 ± 4	21 ± 2	ND	ND	ND
V460M	100 ± 2	16 ± 2	9[e]	53[d]	760[d]
V460S	82 ± 3	21 ± 1	ND	ND	ND
F461W	97 ± 3	23 ± 3	ND	ND	ND

[a] 100% of complex I content corresponds to 1.25 μmol·min^{-1}·mg^{-1} NADH:HAR oxidoreductase activity.
[b] Complex I activity of the parental strain was 0.58 μmol·min^{-1}·mg^{-1}.
[c] Data are from Ref. 21.
[d] Data are from Ref. 14.
[e] Data are from N. Kashani-Poor, unpublished data.
[f] Data are from L. Grgic, unpublished data.

TABLE 2

Effects of point mutations introduced into the PSST subunit

ND indicates not determined.

Strain	Complex I content[a]	Complex I activity[b]	Apparent K_m of DBQ	I_{50} DQA	I_{50} Rotenone
	%	%	μM	nM	
Parental	100 ± 2	100 ± 3	14	13	450
V88F	96 ± 2	13 ± 1	ND	ND	ND
V88L	94 ± 4	92 ± 5	15	25	500
V88M	95 ± 2	56 ± 3	13	32	330
E89A[c]	145	74	19	13	590
E89C[c]	145	67	18	14	630
E89Q[c]	100	88	9	11	620
E185Q[d]	110	35	50	20	500

[a] 100% of complex I content corresponds to 1.25 μmol·min^{-1}·mg^{-1} NADH:HAR oxidoreductase activity.
[b] Complex I activity of the parental strain was 0.6 μmol·min^{-1}·mg^{-1}.
[c] Data are from Ref. 28; here NBQ was use instead of DBQ.
[d] Data are from Ref. 22.

Effects of Point Mutations on EPR-detectable Iron-Sulfur Clusters—To probe for major deformation of the cavity and possible effects on cluster N2, we also recorded EPR spectra of mitochondrial membranes from mutants that showed significant changes in the properties of complex I. In cases where we had made several exchanges in the same position, we analyzed those mutants that exhibited the most drastic effect on activity (supplemental Fig. S2). From previous studies it is known that the shape of the EPR signature of iron-sulfur cluster N2 is highly sensitive to structural changes in its environment (14, 21, 28). Remarkably, in none of the mutations made for this study could we detect significant changes in the EPR spectra of iron-sulfur cluster N2 or any of the other EPR detectable iron-sulfur clusters, irrespective of the reductant used (NADH or NADH/dithionite). This suggested that the structural changes introduced by the mutations were largely local.

Effects of Point Mutations on Complex I Ubiquinone Reductase Activity—In a number of mutants we observed significant reductions of the specific inhibitor-sensitive ubiquinone reductase activity of complex I (Tables 1 and 2). By introducing multiple exchanges in a given position, we probed how critically catalytic activity depended on the size and properties of a particular side chain. Although in some regions of the 49-kDa subunit different exchanges had comparatively severe effects on activity, in other parts of the protein only some of the mutations markedly reduced activity. Compared with mitochondrial membranes from the parental strain, mutagenesis of residues Ala-94, Val-97, Leu-98, Arg-99, and Tyr-144 reduced specific ubiquinone reductase activity dramatically to values that were below 25% in all cases. In contrast, exchanging the hydrophobic residue with a much smaller hydrophilic residue in mutant V145T had virtually no effects, whereas mutation V145F markedly reduced complex I activity. Also for Arg-141 the changes in activity depended on the amino acid that was introduced (14, 21), and in position 407 only the drastic exchange K407W strongly impaired activity, whereas the more conservative exchanges K407H or K407R had only moderate or no effect. Marked reductions of catalytic activity were also observed with mutations M188Y and S192Y and for several mutations near the C terminus of the 49-kDa subunit between residues 455 and 461.

Of the mutations within the PSST subunit, only V88F strongly reduced the specific ubiquinone reductase activity. Mutation E185Q that we had analyzed in earlier studies (22) and mutation V88M had only moderate effects on activity.

To see how the severity of effect of the different mutations correlated with their location in the cavity, we grouped and color-coded them into four categories (Fig. 2); in some positions mutagenesis resulted in activities that were comparable with the parental strain (>75%, *blue*), and in others, the mutant activities were markedly reduced (25–75%, *green*). Yellow was used if at least one mutant with an activity below 25% was found. If several exchanges all resulted in complex I activities below <25% of the parental strain, this was indicated by *red* color. A color-coded representation of our results in the structure around cluster N2 (Fig. 2) illustrates that the effects of the mutations nicely correlated with their positions within the ubiquinone binding cavity. The most severe reductions of activ-

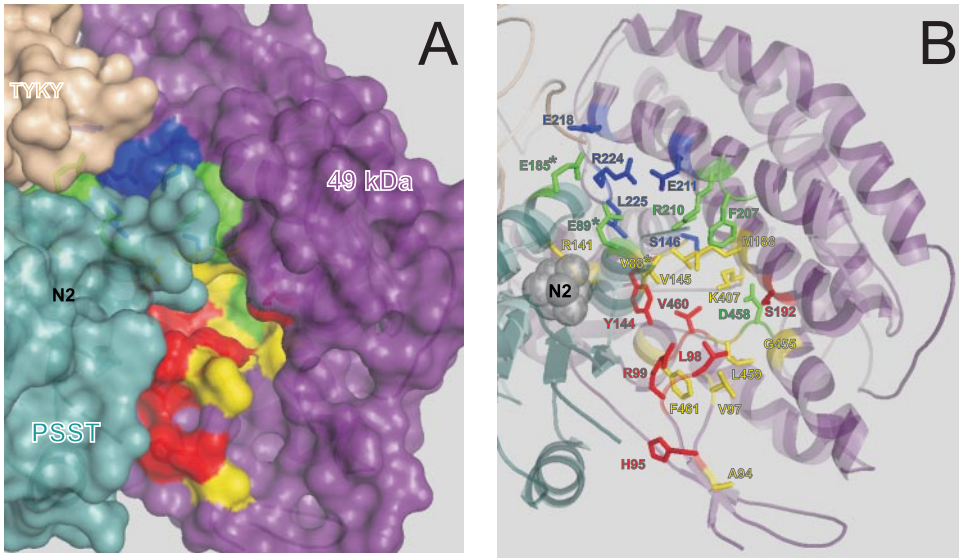

FIGURE 2. **Effects of point mutations on complex I activity.** The putative ubiquinone binding cavity of complex I is shown as a schematic with exchanged amino acids highlighted in *stick* representation. Amino acids mutated within the putative quinone binding cavity are color-coded to illustrate the effect on dNADH: ubiquinone oxidoreductase activity observed for an amino acid exchange in a given position in complex I from *Y. lipolytica*. *Red*, several exchanges all resulted in very low activity (<25% of parental); *yellow*, at least one exchange resulted in very low activity (<25% of parental); *green*, reduced activity (between 25 and 75% of parental); *blue*, essentially normal activity (>75% of parental) for all exchanges. Residues of subunit PSST are marked with an *asterisk*. Iron-sulfur cluster N2 is shown as *gray spheres*. *A*, surface representation. *B*, schematic representation.

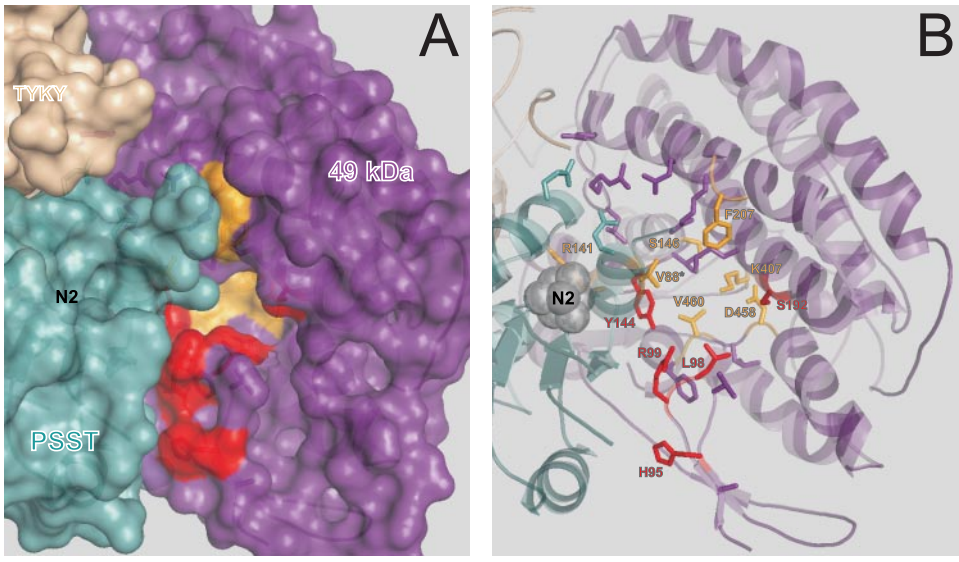

FIGURE 3. **Effects of point mutations on I_{50} value of complex I inhibitors.** The same view into the ubiquinone binding cavity of complex I as in Fig. 2 is shown. However, amino acids that, when exchanged, had an effect on I_{50} of DQA or rotenone are now shown in *orange*. For better orientation, other residues that were most critical for catalytic activity are shown again in *red*. The other mutated residues highlighted in Fig. 2 are now shown in the same color as the secondary structure schematic of the subunit. (*A* and *B* as in Fig. 2).

ity were observed along a path leading from the first strand of the N-terminal β-sheet of the 49-kDa subunit toward a region adjacent to iron-sulfur cluster N2.

Effects of Point Mutations on Apparent K_m Value for DBQ—To test whether the mutations had altered the ubiquinone-binding site of complex I, we determined their apparent K_m value for the ubiquinone derivative DBQ (Tables 1 and 2). However, this was only possible for those mutants that had a residual activity of well above 20% of the parental strain. Many mutants exhibited a slightly lower apparent K_m value than the parental strain, but in most cases this seemed to go parallel with reduced ubiquinone reductase activity, a trend that we had observed previously with complex I mutations. Overall none of the mutants analyzed here that had retained appreciable ubiquinone reductase activities exhibited marked changes in the apparent K_m value for DBQ.

Effects of Point Mutations on I_{50} of Specific Complex I Inhibitors—Many different complex I inhibitors are known that act on the quinone-binding site. Because of their kinetic properties these inhibitors are divided into three classes, A–C (19), with different but partially overlapping binding sites (29). Because DQA and rotenone are very potent representatives of class A and B, respectively, we measured the I_{50} values for these inhibitors in our complex I mutants. Again, reliable determination of this parameter was only possible if the residual activity of a given mutant was well above 20%. Mutation K407R in the 49-kDa subunit caused a 4.7-fold increase of the I_{50} value for DQA, but no change in the I_{50} value for rotenone. In contrast, for mutant F207W we observed a significant increase in the I_{50} value only for rotenone. Mutation V88M in the PSST subunit exhibited a slight hypersensitivity for rotenone and some resistance to DQA. The latter was also observed to a somewhat lesser extent in PSST mutant V88L. All other mutants studied here exhibited I_{50} values for both inhibitors that were not significantly different from the parental strain (Table 1 and 2). Table 1 also contains several previously generated and published mutations, which change I_{50} for DQA and rotenone. All resistance data are illustrated in Fig. 3. Amino acid positions where mutants exhibited resistance or hypersensitivity to DQA or rotenone are shown in *orange* in Fig. 3. For orientation, the residues that were most critical for catalytic activity are shown again in *red* in Fig. 3.

DISCUSSION

We have probed the proposed ubiquinone binding cavity within the peripheral arm of complex I by site-directed mutagenesis. Of the 39 mutations that were analyzed here, a

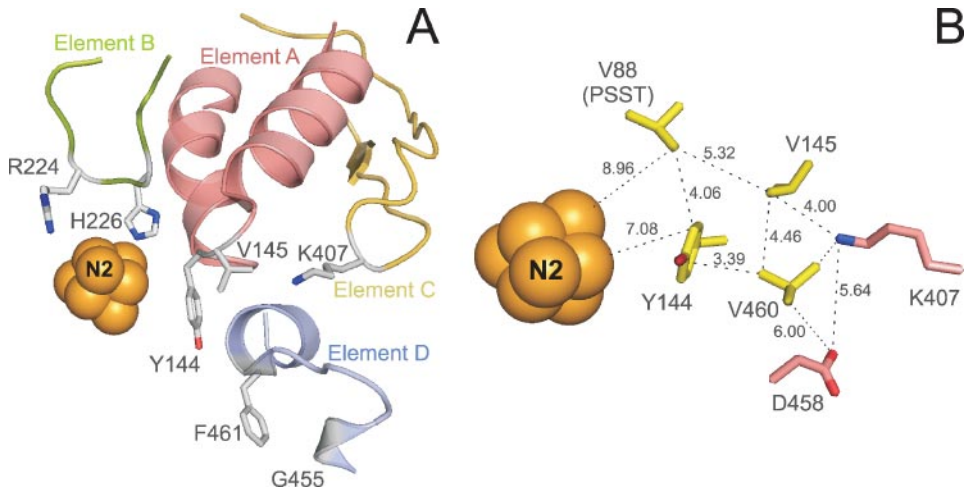

FIGURE 4. **Functionally important residues in the vicinity of iron-sulfur cluster N2.** *A,* mutated residues within the conserved fold around iron-sulfur cluster N2. Structural elements *A–D* had been previously defined based on the homology between complex I and soluble [NiFe] hydrogenases (31). Residues discussed in the text are shown as *stick models. B,* hydrophobic platform around Tyr-144. Only the side chains are shown as *stick models.* Hydrophobic residues are shown in *yellow.* Two hydrophilic residues nearby are shown in *pink.* Distances are given in ångströms. See text for further details.

significant number resulted in a marked reduction of inhibitor-sensitive ubiquinone reductase activity. Several mutations changed inhibitor sensitivity. By localizing the corresponding residues in the partial structure of complex I from *T. thermophilus* (18) and by combining these results with information from earlier studies (14, 21, 28), we could identify functionally important regions within this central domain of complex I (Figs. 2 and 3). The region identified as being most critical for activity included a group of residues that (except for Tyr-144, Ser-192, and Val-460) were not located immediately in the spacious cavity around cluster N2 but rather seemed to form a path of entry for ubiquinone (Fig. 2*A*). This path starts with Ala-94 at a distance of about 24 Å from the ubiquinone-reducing iron-sulfur cluster N2 within the first strand of the N-terminal three-stranded β-sheet of the 49-kDa subunit. The amphipathic loop connecting the first and second strand of this β-sheet reaches into the proposed ubiquinone binding pocket. All five mutations that we introduced here for the three consecutive, highly conserved residues Val-97, Leu-98, and Arg-99 drastically reduced ubiquinone reductase activity (Table 1). Already in an earlier study (21), we had found that all three exchanges we had introduced for the neighboring residue His-95 also abolished complex I activity. The same was found for His-91, which seems to reside in a region that is disordered in the isolated peripheral arm as it is not contained in the *T. thermophilus* structural model (18). This high density of functionally important residues strongly suggested that the N-terminal β-sheet represents a critical part of the ubiquinone binding pocket of complex I.

Somewhat deeper into the crevice but on its opposite side, we could identify another region, where amino acid exchanges M188Y and S192Y significantly impaired catalytic activity (Fig. 2). These residues are located within the lower half of a four α-helical bundle that could be called the backbone of the ubiquinone binding pocket. Remarkably, mutagenesis of a group of strictly conserved and polar residues in the most remote part of the cavity (Glu-211, Glu-218, and Arg-224) and of Leu-225 had virtually no effect on activity or inhibitor binding (Fig. 2).

Based on the homology between the 49-kDa and PSST subunits of complex I and the large and small subunits of [NiFe] hydrogenase, we had previously identified conserved structural elements in the 49-kDa subunit (31) that were now confirmed by the high resolution structure of the peripheral arm to form a conserved fold around iron-sulfur cluster N2 (18). Our results reported here support our proposal that this fold (Fig. 4*A*) in fact forms an important part of the ubiquinone reducing catalytic core of complex I (14). Mutations V145F and Y144W and the earlier described mutation Y144H (14) reside in the loop connecting the two α-helices that form element A and resulted in loss of ubiquinone reductase activity. Element A lines the interface between the 49-kDa subunit and the iron-sulfur subunits PSST and TYKY. Remarkably, mutagenesis of Val-88 in the PSST subunit that is located at only about 4 Å distance from Tyr-144 and Val-145 resulted in loss of activity when a bulky phenylalanine was introduced (Table 2). In contrast, mutation V88M resulted in an about 2–3-fold resistance to DQA and slight hypersensitivity to rotenone suggesting that substrate and inhibitor binding are closely linked in this region of the pocket.

Exchanging the fully conserved Arg-224 that resides within the long disordered loop of element B (Fig. 4*A*) had no significant effect on catalytic activity. Note however, that His-226 found at the tip of the hairpin loop of element B is the redox-Bohr group of cluster N2 (20). Lys-407 is situated on a loop forming element C that is arranged in parallel to element A (Fig. 4*A*). Mutation K407W caused a marked reduction in ubiquinone reductase activity, whereas mutation K407R resulted in an almost 5-fold resistance toward DQA. Note that in this position an arginine is found in *T. thermophilus.* Element D is a highly conserved mostly random coil C-terminal stretch that approaches the region around cluster N2 from the side opposite to elements A and C. It hosts several previously reported mutations (12, 13, 14) that lead to marked inhibitor resistance or, like mutations F461W and G455I studied here, to reduced catalytic activity.

A more detailed analysis of the effect of the mutations on the conserved fold around iron-sulfur cluster N2 revealed a remarkable structural feature that may well play a central role in the catalytic mechanism of complex I; a triad of three hydrophobic residues, Val-88 in the PSST subunit and Val-145 and Val-460 in the 49-kDa subunit that are spaced only a few ångströms from each other, seem to form a hydrophobic platform around Tyr-144 (Fig. 4*B*). Tyr-144 has been shown previously to be critical for ubiquinone reduction (14) and is only about 7 Å away from cluster N2. Although mutating Val-460 to alanine resulted in complete loss of activity, introduction of a bulky

aromatic side chain was required to achieve similar effects at positions Val-88 and Val-145. In position Val-460 and a number of positions nearby, mutations could be found that conferred resistance to hydrophobic inhibitors of complex I. These include the previously found mutations V460M and D458A (14) and mutation K407R from this study. Many mutations in this region also exhibited a significantly reduced ubiquinone reductase activity. Overall, our findings experimentally confirm earlier concepts that the substrate ubiquinone binds in a pocket near iron-sulfur cluster N2 that also comprises the binding sites for the hydrophobic inhibitors of complex I (14, 29). Although the specific binding sites for ubiquinone and the different inhibitors are not identical, they clearly seem to overlap extensively. Another remarkable feature of this extended binding domain is that it can be divided into a hydrophobic region around Tyr-144 and a hydrophilic region formed by Lys-407 and Asp-458 at the C-terminal end of the 49-kDa subunit (Fig. 4*B*).

From the structural model of the peripheral arm of *T. thermophilus* complex I, the entrance of the ubiquinone pocket that can now be defined more precisely by the results reported here can be subdivided into functionally different regions. However, given the large number of functionally critical residues in this region, it seems possible that in intact complex I this region is much more compact, forming a rather narrow amphipathic pathway for the substrate.

It has been a controversial issue where the ubiquinone reduction site is located relative to the membrane surface (30). Although this study does not directly address this question, it should be noted that the β-sheet forming the entry of the ubiquinone pathway defined here contains as its middle strand the epitope that binds a monoclonal antibody in native complex I (30). This implies that this β-sheet must reside close to the surface of the multiprotein complex. We had localized this epitope by electron microscopic analysis of antibody decorated complex I particles at a position far above the presumed level of the inner mitochondrial membrane (30). This unexpected position is supported by a more recent study where we could model the x-ray structure of the peripheral arm of *T. thermophilus* complex I into a three-dimensional model of *Y. lipolytica* complex I obtained by electron microscopic single particle analysis (32). It would follow from these studies that the ubiquinone-reducing iron-sulfur cluster N2 resides 60 Å above the membrane surface and that the ubiquinone binding crevice opens to the water phase and not the membrane. Long known properties of complex I also support this view. In stark contrast to the cytochrome bc_1 complex, for example, hydrophilic ubiquinone analogues like ubiquinone-1 are excellent substrates for complex I (1). Moreover, even charged compounds like *N*-methyl-4-phenylpyridinium can reach the ubiquinone reduction site and inhibit complex I (19). Conserved polar residues within the identified path may also play a role in proton access to the pocket.

It seems however hard to envision how the extremely hydrophobic substrate ubiquinone-10 and the hydrophobic inhibitors could reach a binding site that resides far above the level of the membrane. One option would be that complex I undergoes extensive conformational changes during turnover that brings the ubiquinone binding pocket down to the membrane. Another option would be that the peripheral domains of some of the membrane-bound subunits and the PSST subunit form a ramp or channel that could shuttle the substrate between the membrane domain and the ubiquinone binding pocket. Based on the orientation of the pocket predicted from our structural studies (32), it is tempting to speculate that the long ubiquinone tail acts as a tether that slides along this ramp or channel, whereas the headgroup of the substrate diffuses through the water phase. Solving a high resolution structure of the entire complex will be necessary to decide whether such an unusual substrate binding mode is operational in complex I.

Acknowledgment—We thank Gudrun Beyer for excellent technical assistance.

REFERENCES

1. Brandt, U. (2006) *Annu. Rev. Biochem.* **75,** 69–92
2. Leonard, K., Haiker, H., and Weiss, H. (1987) *J. Mol. Biol.* **194,** 277–286
3. Guenebaut, V., Schlitt, A., Weiss, H., Leonard, K., and Friedrich, T. (1998) *J. Mol. Biol.* **276,** 105–112
4. Grigorieff, N. (1998) *J. Mol. Biol.* **277,** 1033–1046
5. Djafarzadeh, R., Kerscher, S., Zwicker, K., Radermacher, M., Lindahl, M., Schägger, H., and Brandt, U. (2000) *Biochim. Biophys. Acta* **1459,** 230–238
6. Böttcher, B., Scheide, D., Hesterberg, M., Nagel-Steger, L., and Friedrich, T. (2002) *J. Biol. Chem.* **277,** 17970–17977
7. Peng, G., Fritzsch, G., Zickermann, V., Schägger, H., Mentele, R., Lottspeich, F., Bostina, M., Radermacher, M., Huber, R., Stetter, K. O., and Michel, H. (2003) *Biochemistry* **42,** 3032–3039
8. Sazanov, L. A., Carroll, J., Holt, P., Toime, L., and Fearnley, I. M. (2003) *J. Biol. Chem.* **278,** 19483–19491
9. Radermacher, M., Ruiz, T., Clason, T., Benjamin, S., Brandt, U., and Zickermann, V. (2006) *J. Struct. Biol.* **154,** 269–279
10. Böhm, R., Sauter, M., and Böck, A. (1990) *Mol. Microbiol.* **4,** 231–243
11. Albracht, S. P. J. (1993) *Biochim. Biophys. Acta* **1144,** 221–224
12. Darrouzet, E., Issartel, J. P., Lunardi, J., and Dupuis, A. (1998) *FEBS Lett.* **431,** 34–38
13. Prieur, I., Lunardi, J., and Dupuis, A. (2001) *Biochim. Biophys. Acta* **1504,** 173–178
14. Kashani-Poor, N., Zwicker, K., Kerscher, S., and Brandt, U. (2001) *J. Biol. Chem.* **276,** 24082–24087
15. Loeffen, J., Elpeleg, O., Smeitink, J., Smeets, R., Stöckler-Ipsiroglu, S., Mandel, H., Sengers, R., Trijbels, F., and Van den Heuvel, L. (2001) *Ann. Neurol.* **49,** 195–201
16. Schuler, F., Yano, T., Di Bernardo, S., Yagi, T., Yankovskaya, V., Singer, T. P., and Casida, J. E. (1999) *Proc. Natl. Acad. Sci. U. S. A.* **96,** 4149–4153
17. Kerscher, S., Kashani-Poor, N., Zwicker, K., Zickermann, V., and Brandt, U. (2001) *J. Bioenerg. Biomembr.* **33,** 187–196
18. Sazanov, L. A., and Hinchliffe, P. (2006) *Science* **311,** 1430–1436
19. Degli Esposti, M. (1998) *Biochim. Biophys. Acta* **1364,** 222–235
20. Zwicker, K., Galkin, A., Dröse, S., Grgic, L., Kerscher, S., and Brandt, U. (2006) *J. Biol. Chem.* **281,** 23013–23017
21. Grgic, L., Zwicker, K., Kashani-Poor, N., Kerscher, S., and Brandt, U. (2004) *J. Biol. Chem.* **279,** 21193–21199
22. Garofano, A., Zwicker, K., Kerscher, S., Okun, P., and Brandt, U. (2003) *J. Biol. Chem.* **278,** 42435–42440
23. Chen, D.-C., Beckerich, J.-M., and Gaillardin, C. (1997) *Appl. Biochem. Biotechnol.* **48,** 232–235
24. Kerscher, S., Okun, J. G., and Brandt, U. (1999) *J. Cell Sci.* **112,** 2347–2354
25. Eschemann, A., Galkin, A., Oettmeier, W., Brandt, U., and Kerscher, S. (2005) *J. Biol. Chem.* **280,** 3138–3142
26. Schägger, H. (2003) in *Membrane Protein Purification and Crystallization:*

A Practical Guide (Hunte, C., von Jagow, G., and Schägger, H., eds) pp. 105–130, Academic Press, San Diego
27. Wittig, I., Karas, M., and Schagger, H. (2007) *Mol. Cell. Proteomics* **6,** 1215–1225
28. Ahlers, P., Zwicker, K., Kerscher, S., and Brandt, U. (2000) *J. Biol. Chem.* **275,** 23577–23582
29. Okun, J. G., Lümmen, P., and Brandt, U. (1999) *J. Biol. Chem.* **274,** 2625–2630
30. Zickermann, V., Bostina, M., Hunte, C., Ruiz, T., Radermacher, M., and Brandt, U. (2003) *J. Biol. Chem.* **278,** 29072–29078
31. Kerscher, S., Zickermann, V., Zwicker, K., and Brandt, U. (2005) in *Biophysical and Structural Aspects of Bioenergetics* (Wikstrom, M., ed) pp. 156–184, Royal Society of Chemistry, Cambridge, UK
32. Clason, T., Zickermann, V., Ruiz, T., Brandt, U., and Radermacher, M. (2007) *J. Struct. Biol.,* in press